ISSN 1330–0008
CODEN FIZAE4

STRUCTURAL AND ELECTRONIC PROPERTIES OF bcc SELENIUM UNDER HIGH PRESSURE

FOUAD EL HAJ HASSAN[1], MOUHAMED ZOAETER and ABBAS HIJAZI

Université libanaise, Faculté des sciences (I), Laboratoire de physique de matériaux (LPM), Elhadath, Beirut, Lebanon

Received 25 August 2004; revised manuscript received 15 February 2005
Accepted 6 June 2005 Online 6 February 2006

Full-potential linearized augmented plane-wave method (FP-LAPW) within the density functional theory is applied to study the structural and electronic properties of selenium in the bcc phase at high pressures. We used local density approximation with and without generalized gradient correction based on exchange-correlation energy optimization. We have determined the full set of first-order elastic constants, which have not been established earlier experimentally or theoretically. The elastic moduli show linear dependence on pressure. The calculated energy allowed us to investigate several structural properties such as lattice parameter, bulk modulus and its pressure derivative. Our calculated lattice parameter is found to be in reasonable agreement with experimental result. The electronic band structure and the density of states at various pressures are also calculated to show that there is a possibility for these compounds to become metallic at high pressures. Further, we have calculated the electronic specific heat coefficient, which decreases with the increase of pressure.

PACS numbers: 62.20.Dc, 71.15.Mb, 71.15.-m, 71.15.Nc, 71.20.-b UDC 539.3

Keywords: selenium, FP-LAPW, high pressure, bcc phase, elastic constant, band structure, density of states

1. Introduction

Recently, there has been a growing interest in the study of materials under high-pressure conditions, motivated by the need of synthesizing new solids with targeted physical properties [1] and animated by the availability of improved experimental techniques [2]. In this context, renewed attention has been given to the group-VIb elements, O, S, Se, and Te, which exhibit very interesting properties under pressure. The group-VIb elements selenium and tellurium show a similarity in their

[1]Corresponding author: E-mail address: hassan.f@ul.edu.lb, Tel: 00 961 5 460494, Fax: 00 961 5 461496

properties, they are semiconductors at ambient pressure but transform to metallic phase and exhibit superconductivity under high pressure. The stable form of this element is hexagonal and consists of spiral chains parallel to the c-axis [3, 4].

Previous high-pressure X-ray diffraction studies of Te have shown that hexagonal Te undergoes four structural phase transitions with increasing pressure from its most stable hexagonal phase to a monoclinic phase at 4.5 GPa [4], to an orthorhombic phase at 6 GPa [4], to a β-Po-type structural phase at 11 GPa [5] and finally to the higher-symmetry bcc structure at 27 GPa [6]. In analogy with Te, one could expect that Se might also exhibit a similar sequence of structural phase transition as tellurium. Recent X-ray diffraction study on Se up to 50 GPa [7] shows three structural phase transitions: from hexagonal to monoclinic at 14 GPa, to tetragonal at 28 GPa and to rhombohedral at 41 GPa. Energy dispersive X-ray diffraction studies [8] identified the structure of Se IV (63 GPa) as β-Po-type with one atom in the rhombohedral unit cell and thus in close similarity to Te under pressure. The most recent X-ray diffraction study [9] on Se in the extended pressure range up to 150 GPa shows the following sequences of structural phase transitions, from a hexagonal (Se-I) to an intermediate (Se-I) phase at 14 GPa, to a monoclinic (Se-III) phase at 23 GPa, to an orthorhombic (Se-IV) phase at 28 GPa, to a β-Po-type-structure (Se-V) phase at 60 GPa, and finally to a bcc (Se-VI) phase at 140 GPa.

Theoretical calculations have been employed to examine the electronic structure of selenium with a view to exploring successive pressure-driven transition [10] and the appearance of superconductivity [11]. The total energy calculations in both the hexagonal and β-Po-type phase have been also carried out [12, 13]. In the full-potential linearized-plane-wave method used by Geshi et al. [14], the calculated transition pressure is severely underestimated with respect to the experimental value. Recently, the structural phase diagrams, phonon spectra and electron-phonon coupling are compared at high-pressure structural phase of S and Se using plane-wave pseudopotential method [15]. The structural and superconducting transition of two high-pressure phases of solid selenium, β-Po and bcc, has been theoretically investigated using the full-potential linearized muffin-tin orbital (FPLMTO) method [16].

The purpose of this paper is to apply the full-potential linearized augmented plane-wave (FP-LAPW) method to calculate the elastic properties of Se in the bcc phase. We have determined the full set of first-order elastic constant, which to best of our knowledge have not been previously established experimentally or theoretically. This will be followed by a detailed presentation of the band structure and the density of states (DOS). This paper is organized as follows: in Sect. 2, we briefly give the computational details, results and discussion are presented in Sect. 3 and Sect. 4 presents the conclusion.

2. Computational details

The calculations were performed using the FP-LAPW approach [17] within the framework of the density functional theory (DFT) [18] as implemented in the

WIEN2K code [19]. The exchange-correlation potential was calculated by local density approximation (LDA) [20] with and without generalized gradient approximation (GGA) based on Perdew et al. [21]. Kohn-Sham wave functions were expanded in terms of spherical harmonic functions inside of non-overlapping muffin-tin spheres surrounding the atomic sites (MT spheres) and in Fourier series in the interstitial region. In the muffin-tin spheres of radius R_{MT}, the l-expansion of the non spherical potential and charge density were carried out up to $l_{\max} = 10$. We considered electrons in [Ar](3d)10 states as core electrons, which were treated as relaxed. In order to achieve convergence of energy eigenvalues, the wave functions in the interstitial region were expanded in plane waves with a cut-off at $K_{\max} = 7/R_{\mathrm{MT}}$. R_{MT} values are assumed to be 2.0 a.u. A mesh of 100 special k-points (grid of 14×14×14) were taken in the irreducible wedge of the Brilloiun zone to calculate the total energy and the band structure, while we have used a mesh of 165 special k-points (grid of 17×17×17) to calculate the elastic moduli. Both the muffin-tin radius and the number of k-points are varied to ensure total energy convergence. In order to consider the relativistic effects in our calculation, the electronic states were classified into two categories, the core and valence states. The core states that are completely confined inside the corresponding muffin-tin spheres are treated fully relativistic. For the valence states that are rather non-localized, we used the scalar relativistic approach that includes the mass velocity and Darwin s-shift, but omits spin-orbit coupling.

3. Results and discussion

Figure 1 shows the total energy of Se bcc structure as a function of volume. The curve was obtained by calculating the total energy E_{T} at many different volumes around equilibrium and by fitting the calculated values to the Murnaghans equation of state (EOS) [22].

$$E_{\mathrm{T}}(V) = \frac{BV}{B'}\left[\frac{(V_0/V)^{B'}}{B'-1}+1\right] + E_0 - \frac{V_0 B}{B'-1}\,, \tag{1}$$

$$B = V\,\frac{\mathrm{d}^2 E_{\mathrm{T}}}{\mathrm{d}V^2}\,, \tag{2}$$

$$P(V) = \frac{B}{B'}\left[\left(\frac{V_0}{V}\right)^{B'} - 1\right], \tag{3}$$

where V and V_0 represent the atomic volume and its value at zero pressure, respectively, B is the bulk modulus and B is the pressure derivative of the bulk modulus.

From this fit, we have calculated the bulk modulus and its pressure derivative using LDA, with and without GGA. In Table 1, we report the calculated equilibrium

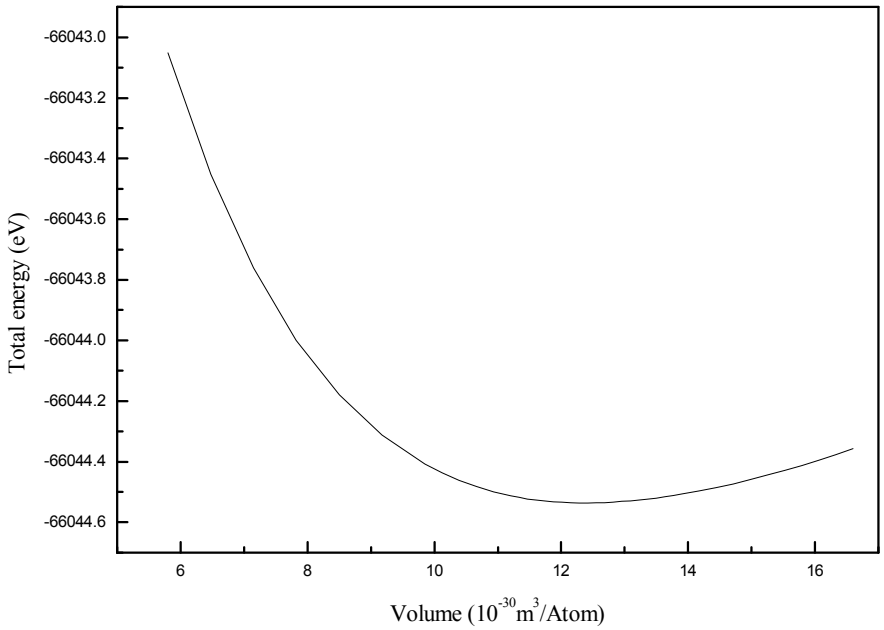

Fig. 1. Total energy as a function of volume for Se *in the* bcc *phase.*

TABLE 1. Calculated lattice constant (a_b) *and the corresponding pressure* (P), *bulk modulus* (B) *and pressure derivatives of bulk modulus* (B) *of* Se *in the* bcc *phase* (Se-VI), *compared to the available experiment work.*

Se-VI		P (GPa)	a_b (10^{-10} m)	B (GPa)	B'
Present	LDA	138	2.794	90.69	5.0
	GGA	122	2.927	99.85	4.6
Experiment [9]		140	2.823		

lattice parameter, corresponding pressure, bulk modulus and the pressure for the Se in bcc phase. The equilibrium lattice constant obtained in the present work without GGA is 0.2927 nm, corresponding to a pressure of 122 GPa. The lattice constant at 140 GPa is 0.2885 nm, which is 2 % higher when compared to the experimental value at the same pressure. Although as a general trend, GGA overestimate the lattice parameter, LDA underestimate it [23 – 26]. It is to be noted that the theoretical calculations were done at $T = 0$ K, whereas the experimental work was performed at the room temperature [27].

To obtain the elastic constants of bcc structure, we have used a numerical first-principles calculation by computing the components of the stress tensor ε for small

strains. It is well known that a cubic crystal has only three independent elastic constants, C_{11}, C_{12} and C_{44}. Hence, a set of three equations is needed to determine all constants, which means that three types of strain must be applied to the starting crystal.

The first type involves calculating the bulk modulus (B), which is related to the elastic constant by [28]

$$B = \frac{1}{3}\left(C_{11} + 2C_{12}\right) . \tag{4}$$

The second type involves performing volume-conservative tetragonal strain tensor $\overleftrightarrow{\varepsilon}$

$$\overleftrightarrow{\varepsilon} = \begin{pmatrix} \varepsilon & 0 & 0 \\ 0 & \varepsilon & 0 \\ 0 & 0 & \dfrac{1}{1+\varepsilon^2} - 1 \end{pmatrix} . \tag{5}$$

Application of this strain has an effect of the total energy from its value as follows

$$E(\varepsilon) = \left(C_{11} - C_{12}\right) 6V\varepsilon^2 + O(\varepsilon^3) , \tag{6}$$

where V is the volume of the unit cell.

Finally, for the last type of deformation, we use the volume-conserving rhombohedral strain tensor given by

$$\overleftrightarrow{\varepsilon} = \frac{\varepsilon}{3}\begin{pmatrix} 1 & 1 & 1 \\ 1 & 1 & 1 \\ 1 & 1 & 1 \end{pmatrix} , \tag{7}$$

which transforms the total energy to

$$E(\varepsilon) = \frac{V}{3}(C_{11} + 2C_{12} + 4C_{44})\varepsilon^2 + O(\varepsilon^3) . \tag{8}$$

The calculation of an elastic modulus C_{ij} from total energy calculations begins by choosing a set of M points ε_i, $(i = 1, 2, \ldots M)$, typically we choose $M = 5$, with $\varepsilon_1 = 0$ and $\varepsilon_5 \approx 0.05$. These three equations form the set of equations needed to determine the full elastic tensor.

The well-known Born stability criteria [29] are a set of conditions on the elastic constants (C_{ij}) which are valid for the special case of zero stress. The elastic stiffness tensor c_{ij} provides a generalization of the zero-stress elastic constant tensor valid under stress [30]. For a cubic crystal under hydrostatic pressure, the generalized elastic stability criteria [31], in analogy to the conventional Born criteria, are

$$c_{11} + 2c_{12} > 0 , \qquad c_{44} > 0 , \qquad c_{11} - c_{12} > 0 . \tag{9}$$

In the case of hydrostatic pressure, the c_{ij} (in the Voigt notation) are related to the C_{ij} defined with respect to the Eulerian strain variables by

$$c_{11} = C_{11}\,, \qquad c_{12} = C_{12} + P\,, \qquad c_{44} = C_{44} - P/2\,. \tag{10}$$

In Fig. 2, we display the variation of c_{11}, c_{12} and c_{44} as function of pressure. A linear behavior appears for all variations. However, a positive slope is noticed for c_{11} and c_{44}, while for c_{12}, the slope is negative. The calculated values for the elastic stiffness coefficients, c_{11}, c_{12} and c_{44}, of the Se compound at equilibrium lattice constant in the bcc phase using LDA with and without the GGA scheme are listed in Table 2. It is clearly seen that our GGA results differ by 5 % from the LDA ones.

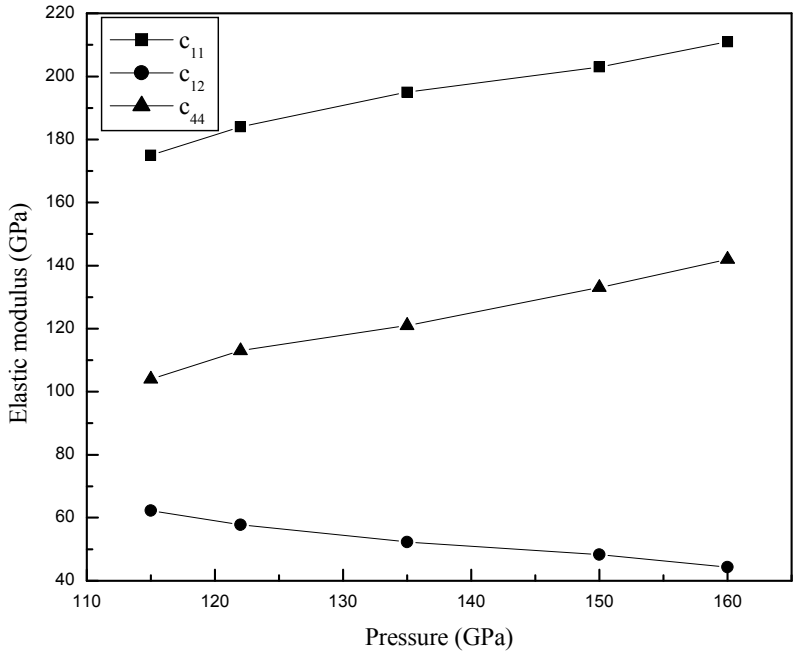

Fig. 2. The pressure variation of c_{11} (solid squares), c_{12} (solid circles) and c_{44} (solid triangles) for the bcc *phase of* Se *using GGA.*

TABLE 2. Calculated elastic constant parameters of Se *in the* bcc *phase at equilibrium lattice constant, corresponding to pressures 138 and 122 GPa, using LDA and GGA, respectively.*

Se-VI		c_{11} (GPa)	c_{12} (GPa)	c_{44} (GPa)
Present	LDA	147.2	62.4	110.2
	GGA	184.0	57.8	113.0

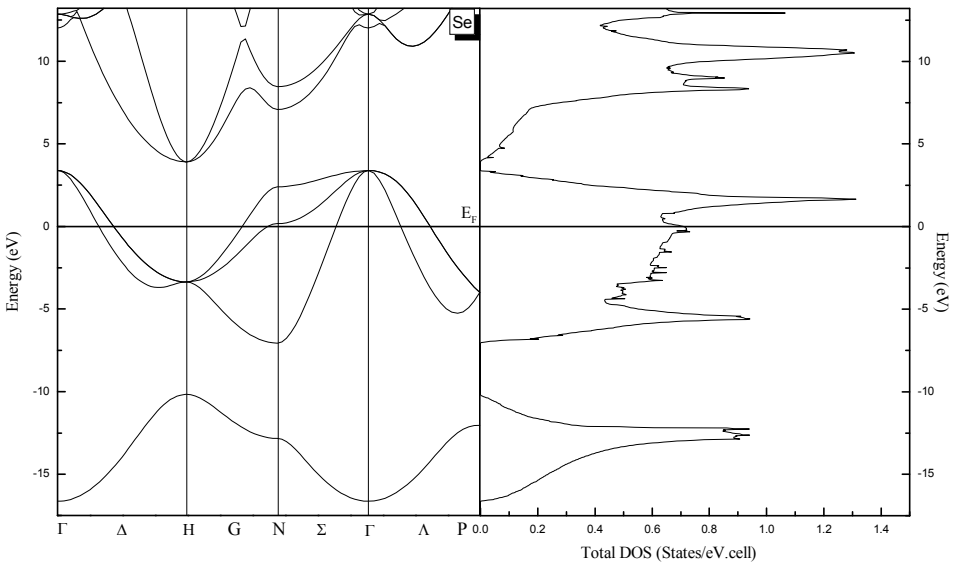

Fig. 3. Band structure along the principal high-symmetry points and the total DOS of Se *in the* bcc *phase.*

The self-consistent band structures of Se were calculated in bcc phase at equilibrium volume within the GGA scheme (Fig. 3). The profile of this band is in agreement with the earlier work by the FPLMTO method [16]. From this figure, it can seen that bcc Se phase is metallic. Metallization is due to the indirect band gap closing at Γ and H-points. The overall band profile exhibits characteristic features similar to other bcc sp-elements. The band coming in the lowest energy region arises from 4s-atomic orbitals in which all states are occupied. The next higher-energy states are mainly 4p-electrons. The upper bands (conduction band) are mainly caused by antibonding 4p- and 4d-states. The overall profile of total DOS (Fig. 3) histogram is also in good agreement with the previous self-consistent FPLMTO work on the bcc phase [16].

Figure 4 shows the partial densities of states (DOSs). The peaks present in the lower-energy region are mainly due to the 4s-electron, whereas upper region mainly consists of 4p- and 4d-orbitals.

Further, it is seem that the Fermi level is shifting gradually to higher energies with the increase of pressure. This may be due to the increase of electron concentration under pressure. DOS at the Fermi level decreases with an increase of pressure. The conduction bandwidth (which is the difference in energy between Fermi level and lowest eigenvalues corresponding to the Γ-point) is calculated for different pressures. It is well known that with the application of pressure, the width of the conduction band decreases because of the increased overlap between various orbitals. A similar trend is observed here. The conduction bandwidth and DOS at Fermi energy are given in Table 2 for various pressures.

Pressure dependence of the electronic specific-heat coefficient (γ), which is a

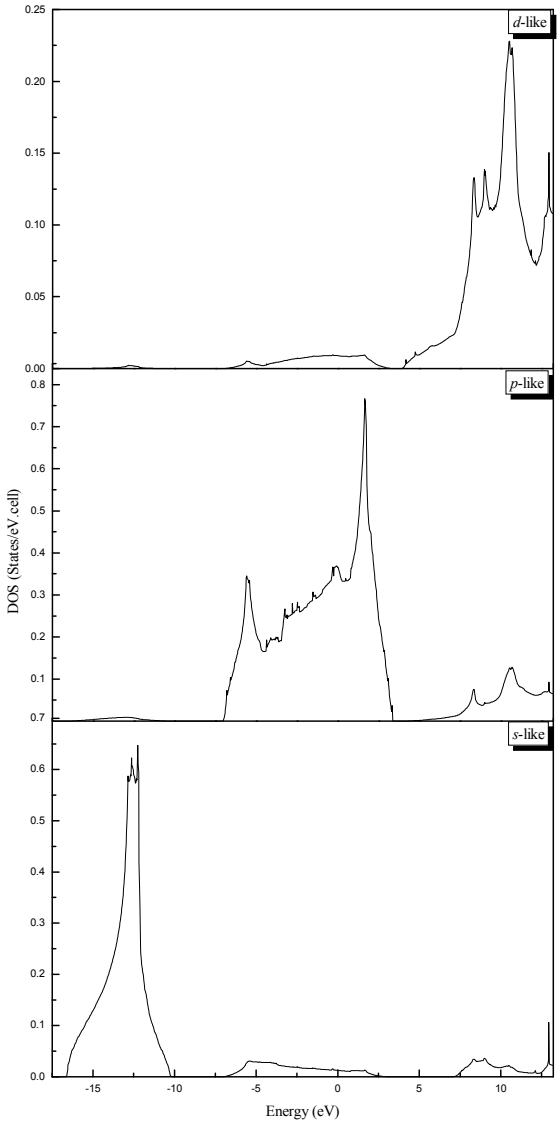

Fig. 4. Calculated partial DOS per formula unit of Se *in the* bcc *phase.*

function of density of states, is calculated using the expression

$$\gamma = \frac{1}{3}\pi^2 N(F_{\mathrm{F}}) k_{\mathrm{B}}^2 N_{\mathrm{A}}\,, \tag{11}$$

Where, $N(F_{\mathrm{F}})$ is the density of states at the Fermi energy, k_{B} is the Boltzmann constant and N_{A} is the Avogadro number. The calculated specific-heat coefficients for different values of V/V_0 are given in Table 3 which shows that it decreases with the increase of pressure.

TABLE 3. Variation of DOS at Fermi energy $N(E_F)$, electronic specific-heat coefficient and conduction band width as a function of V/V_0 in the bcc *phase of* Se.

V/V_0	$N(E_F)$ (states/Ry.cell)	γ (mJ/k^{2}mol)	Band width (eV)
1.00	9.656767	1.67706	16.63736
0.90	8.461574	1.46950	17.74226
0.80	7.327300	1.27251	19.17418
0.70	7.148813	1.24151	20.94880
0.60	5.816449	1.01013	23.44834

4. Conclusions

We have presented a theoretical analysis of the structural and electronic properties of selenium in the bcc phase at high pressures using the FP-LAPW method. We have calculated the total energies as a function of volumes using LDA with and without the GGA scheme. Fitting them with the Murnaghans equation of state allowed us to calculate the equilibrium lattice parameter, bulk modulus and it pressure derivative. A numerical first-principles method was used to predict the elastic constants c_{11}, c_{12} and c_{44}. Additionally, the contribution of every atomic orbital to the electronic structure and the overall band profile were investigated. It is to be noted that there is a possibility for these compounds to become metallic at high pressures. Finally, we have found that the electronic specific-heat coefficient decreases with the increase of pressure.

References

[1] S. C. Schmidt, J. W. Shaner and M. Ross, *High Pressure Science and Technology*, American Institute of Physics, Woodbury, NY (1993).

[2] H. K. Mao and R. J. Hemley, Rev. Mod. Phys. **66** (1994) 671.

[3] R. Keller, W. B. Holzapfel and H. Schulz, Phys. Rev. B **15** (1977) 4404.

[4] K. Aoki, O. Shimomura and S. Minomura, J. Phys. Soc. Japan **48** (1980) 551.

[5] C. Jamieson and D. B. McWhan, J. Chem. Phys. **43** (1965) 1149.

[6] G. Parthasarathy and W. B. Holzapfel, Phys. Rev. B **37** (1988) 8499.

[7] G. Parthasarathy and W. B. Holzapfel, Phys. Rev. B **38** (1988) 10105.

[8] T. Krger, W. B. Holzapfel, Phys. Rev. Lett. **69** (1992) 305.

[9] Y. Akahama, M. Kobayachi and H. Kawamura, Phys. Rev. B **43** (1993) 20.

[10] G. Kress, J. Furthmuller and J. Hafner, Phys. Rev. B **50** (1994) 13181.

[11] F. Mauri, O. Zakharov, S. Gironcoli, S. G. Louie and M. L. Cohen, Phys. Rev. Lett. **77** (1996) 1151.

[12] S. J. Clark, G. J. Ackland and H. Akbarzadeh, J. Phys. Chem. Solids **56** (1995) 329.

[13] A. Nishikawa, K. Niizeki, K. Shindo and K. Ohno, J. Phys. Chem. Solids **56** (1995) 551.

[14] M. Geshi, T. Oda and Y. Hiwatari, J. Phys. Soc. Jpn. **9** (1998) 3141.

[15] S. P. Rudin, A. Y. Liu, J. K. Freericks and A. Quandt, Phys. Rev. B **63** (2001) 224107.

[16] M. Otani and N. Suzuki, Phys. Rev. B **63** (2001) 104516.

[17] D. D. Koelling and B. N. Harmon, J. Phys. C: Sol. State Phys. **10** (1977) 3107.

[18] P. Hohenberg and W. Kohn, Phys. Rev. **136** (1964) 864.

[19] P. Blaha, K. Schwarz, G. K. H. Madsen, D. Kvasnicka and J. Luitz, WIEN2K, an Augmented Plane Wave + Local orbitals program for calculating crystal properties, Karlheinz Schwarz, Techn. Universitat, Wien, Austria, 2001, ISBN 3-9501031-1-2.

[20] W. Kohn and L. J. Sham, Phys. Rev. **140** (1965) 1133.

[21] J. P. Perdew, S. Burke and M Ernzerhof, Phys. Rev. Lett. **77** (1996) 3865.

[22] F. D. Murnaghan, Proc. Natl. Acad. Sci. USA **30** (1944) 5390.

[23] A. Mokhtari and H. Akbarzadeh, Physica B **324** (2002) 305.

[24] A. Zaoui and F. El Haj Hassan, J. Phys.: Condens. Matter **13** (2001) 253.

[25] H. C. Hsueh, C. C. Lee and C. W. Wang, Phys. Rev. B **61** (2000) 3851.

[26] F. El Haj Hassan, H.Akbarzadeh and M. Zoaeter, J. Phys.: Condens. Matter **13** (2004) 293.

[27] P. W. Bridgman, Phys. Rev. **60** (1941) 651.

[28] E. Schreiber, O. L. Anderson and N. Soga, *Elastic Constants and their Measurement*, McGraw-Hill, New York (1973).

[29] M. Born and K. Huang, *Dynamic Theory of Crystal Lattices*, Oxford, Clarendon (1954).

[30] J. Wang, S. Yip, S. Phillpot and D. Wolf, Phys. Rev. B **52** (1995) 12627.

[31] B. B. Karki, G. J. Ackland and J. Crain, J. Phys.: Condens. Matter **9** (1997) 8579.

STRUKTURNA I ELEKTRONSKA SVOJSTVA bbc SELENA POD VISOKIM TLAKOM

Primjenom metode lineariziranih proširenih ravnih valova s potpunim potencijalom, u okviru teorije funkcionala gustoće, proučavali smo strukturna i elektronska svojstva selena u bcc fazi na visokim tlakovima. Primijenili smo približenje lokalne gustoće sa i bez poopćene gradijentne popravke primjenom optimizacije energije korelacije i izmjene. Odredili smo potpun skup elestičnih konstanti prvog reda koje ranije nisu bile određene ni eksperimentalno ni teorijski. Moduli eleastičnosti pokazuju linearnu ovisnost o tlaku. Na osnovi izračunatih energija mogli smo istražiti više strukturnih svojstava, kao što su parametar rešetke, volumni modul stlačivosti i njegova derivacija po tlaku. Naš izračunat parametar rešetke je u dobrom slaganju s eksperimentalnim rezultatom. Također smo izračunali strukturu elekronskih vrpci i gustoće stanja da bismo ukazali na mogućnost da na visokim tlakovima selen u fazi bcc može postati metal. Nadalje, izračunali smo koeficijent elektronske specifične topline koji se smanjuje s porastom tlaka.